

# FAST DETECTION OF SINGLE NANOPARTICLES IN A MICROFLUIDIC CHANNEL BY A MICROLENS ARRAY IN COMBINATION WITH A CONVENTIONAL OPTICAL MICROSCOPE

H. Yang\*, M. Cornaglia and M.A.M. Gijs

*Laboratory of Microsystems, Ecole Polytechnique Fédérale de Lausanne, Switzerland*

## ABSTRACT

We present the use of a microlens array in combination with a conventional optical microscope set-up for the detection of single nanoparticles (NPs) in fluid medium. Optically transparent dielectric microspheres are patterned in a microfabricated well array template and used as microlenses focusing the light originating from a microscope objective into so-called photonic nanojets that expose the medium within the microfluidic channel. When the NPs pass the nanojets, the detection signal is highly enhanced, Au NPs with size down to 50 nm, fluorescent NPs down to 20 nm in size, as well as biomolecule-linked NPs are clearly observed.

**KEYWORDS:** Optical detection, nanoparticle, photonic nanojet

## INTRODUCTION

Conventional optical microscopy only permits detecting NPs that are larger than several hundred nanometers or having extremely enhanced scattering probability, due to the limited scattered light intensity of small NPs and the light collection capability of a low numerical aperture (NA) objective. Advanced optical techniques have been proposed for sensitive detection of nano-objects, but required high-end, expensive, and bulky experimental setups [1]. However, a microsphere is known to act as a focusing microlens, in case the illumination light propagating through the microsphere can be focused into a photonic nanojet. Such nanojet has a highly enhanced intensity and a sub-wavelength ( $\lambda$ ) full-width-at-half-maximum (FWHM) beam width. When the nanojet is used to illuminate a NP, the latter can generate a highly enhanced back-scattering signal for detection [2]. In the demonstrated technique, we firstly positioned at the bottom of a microfluidic channel an array of microspheres that are patterned in a microwell array template. The template is microfabricated in a Parylene-C layer on a glass substrate, which is then reversibly bonded with a polydimethylsiloxane (PDMS) channel [3]. 3  $\mu\text{m}$ -size melamine microspheres are selected as the microlenses due to their optimum light focusing capability in water [4]. As shown in Figure 1, the microspheres focus the light originating from a 20 $\times$  objective into photonic nanojets with FWHM  $\sim$ 240 nm. When a Au NP or a fluorescent NP dispersed in the liquid medium is transported through a nanojet, its back-scattered light (for a bare Au NP) or its fluorescent emission is instantaneously detected by video microscopy via the same objective. A finite element method (FEM) study on the electromagnetic wave propagation is performed; the light intensity distribution in Figure 2a clearly shows the photonic nanojet. When a 50 nm Au NP is transported through the nanojet, the simulation result (Figure 2b) predicts a higher intensity than that from the microsphere alone.

## EXPERIMENTAL

Bare Au NPs in citrate buffer (Sigma-Aldrich) are diluted in de-ionized water, and calibrated fluorescent (Molecular Probes) NPs are dispersed in PBS-Tween 20 (0.5% v/v) buffer into the same concentration of  $1 \times 10^5$  particles/mL. The solution is introduced into the microfluidic channel at a flow velocity of  $\sim$ 10  $\mu\text{m}/\text{sec}$  by a neMESYS syringe pump (Cetoni); this velocity corresponds to 20 milliseconds during which the NPs are typically exposed to the strong intensity of the nanojet. A sample amount of  $\sim$ 300 nL is used in each experiment. An Axiovert S100 inverted microscope is equipped with a 20 $\times$  objective with NA=0.22, a mercury vapor arc lamp and appropriate fluorescent filter sets (Carl Zeiss). Image acquisition and light detection are achieved using a CCD camera (Hamamatsu Photonics).

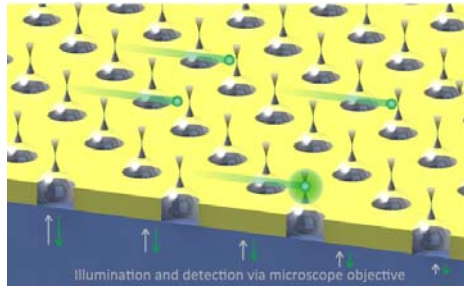


Figure 1: Schematic illustration on the optical detection of NPs. Dielectric microspheres are patterned in a micro-fabricated well template on a glass substrate. A low-NA objective is placed beneath the thus formed microlens array. Illumination light from the objective is focused by each microlens into a photonic nanojet having a sub-diffraction limit beam width. A NP is transported in the microfluidic channel and, when it passes through a nanojet, its back-scattered light is highly enhanced and detected via the same objective.

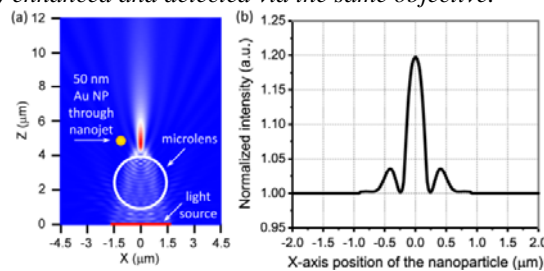


Figure 2: FEM simulation of a 50 nm Au NP passing through a photonic nanojet which is emerging from a microlens. (a) Light intensity distribution clearly shows the nanojet. (b) Normalized intensity (relative to the presence of a microsphere alone) as a function of the position of the NP.

## RESULTS AND DISCUSSION

Firstly Au NPs with different sizes are introduced into the microfluidic channel and detected by bright-field microscopy. The presence of a 400 nm Au NP in the nanojet results in a back-scattered light intensity that is significantly enhanced with respect to that of a NP outside of the nanojet (Figure 3a), and a single Au NP with size down to 50 nm can be observed through the microsphere, as shown in Figure 3b. Figure 3c is a plot of the experimental back-scattered light intensity as function of the NP size, indicating an initial rise followed by a saturated behavior when the size of the Au NP is bigger than the FWHM of the photonic nanojet. By comparing the integrated signal obtained from a 200 nm Au NP inside and outside of the nanojet, a signal enhancement factor of  $\sim 40$  is obtained.

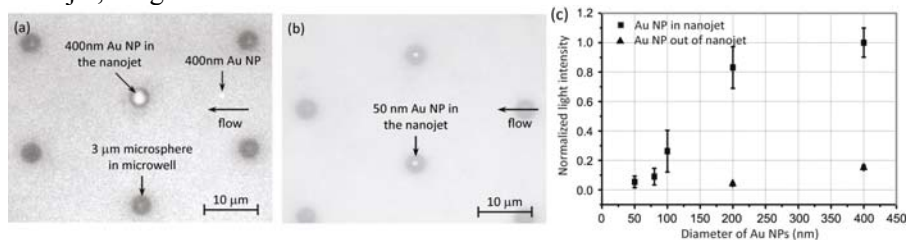


Figure 3: (a,b) Microscopic images of (a) 400 nm and (b) 50 nm Au NPs in the photonic nanojets, respectively. (c) Light intensity of Au NPs, positioned within and outside of a nanojet, as function of the NP size.

Secondly, size-calibrated polystyrene fluorescent NPs with emission wavelength  $\lambda_{em} = 515$  nm are detected via a fluorescent microscope set-up. The fluorescent signal of a 460 nm NP is extremely bright when located in a nanojet (Figure 4a), so that NPs with 20 nm in diameter could be still distinguished when passing through a nanojet (Figure 4b), as the fluorescent emission filter efficiently removed the excitation light and fluorescence at wavelengths other than  $\lambda_{em}$ . A signal enhancement factor of  $\sim 44$  is obtained by comparing the signal from a 190 nm fluorescent NP positioned in and out of the nanojet (Figure 4c).

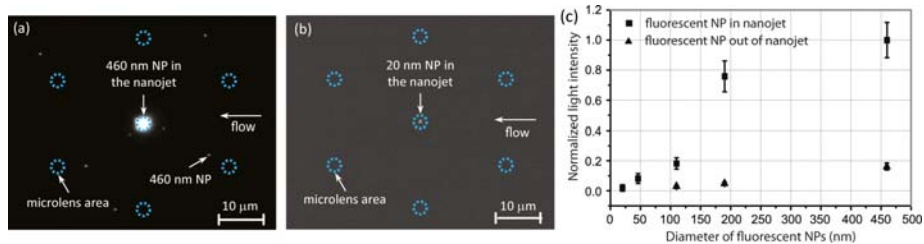


Figure 4: (a,b) Microscopic images of (a) 460 nm and (b) 20 nm fluorescent NPs in the photonic nanojets, respectively. (c) Light intensity of NPs, positioned within and outside of a nanojet, as function of the NP size.

We then demonstrated the potential of our technique for immunodetection of biomolecules. Normal mouse IgG is conjugated to surface-functionalized Au NPs and expressed by a secondary fluorescently labeled anti-mouse IgG. Hereafter, the conjugated Au NPs show highly enhanced fluorescence when transiting through the nanojets (Figure 5), indicating that the detection of biomolecules with weak optical signal intensities can be very efficiently enhanced indeed by the microlens array due to the highly amplified fluorescent excitation field in the photonic nanojet.

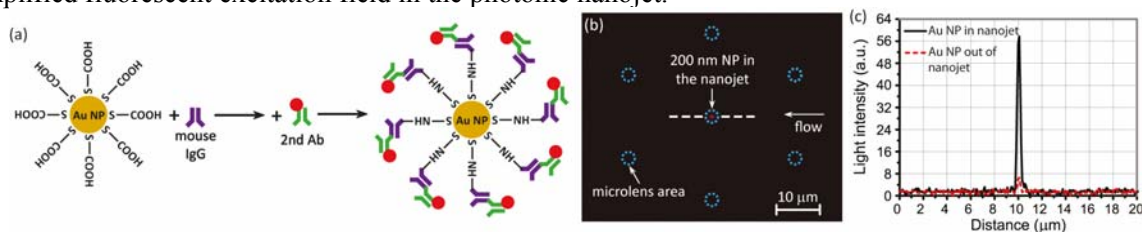


Figure 5: Detection of mouse IgG on functionalized Au NPs using AlexaFluor647-labeled anti-mouse IgG detection antibodies, all spiked in PBS. (a) Schematic two-step conjugation protocol for detection of mouse IgG by functionalized Au NPs. (b) Microscopic image and (c) intensity profile for a 200 nm conjugated Au NP in the nanojet (along the dashed line in (b)), compared with the signal profile of a NP out of the nanojet.

## CONCLUSION

In conclusion, the detection of NPs with a size far below the classical diffraction limit is achieved in a microfluidic device. Our technique exploits the unique properties of a photonic nanojet. When NPs are transported through a nanojet over 20 milliseconds, their light scattering or fluorescence intensity is typically enhanced by a factor  $\sim 40$ . This approach could evolve in a novel tool to detect a wide-class of nano-objects in liquids, or for monitoring synthesis and aggregation processes on a molecular level.

## ACKNOWLEDGEMENTS

The authors would like to thank the European Research Council (ERC-2012-AdG-320404) and the Swiss National Science Foundation (200020-140328) for providing the funding of this work.

## REFERENCES

- [1] J. Zhu, *et al.*, "On-chip single nanoparticle detection and sizing by mode splitting in an ultrahigh-Q microresonator," *Nature Photon.*, 4, 46-49, 2010.
- [2] H. Yang, M. Cornaglia, and M.A.M. Gijs, "Photonic nanojet array for fast detection of single nanoparticles in a flow," *Nano Lett.*, 15, 1730-1735, 2015.
- [3] H. Yang, M. Cornaglia, and M.A.M. Gijs, "Lens array by electrostatic patterning of dielectric microspheres in a Parylene-C well template," *Proceedings of Micro Total Analysis Systems 2014*.
- [4] H. Yang and M.A.M. Gijs, "Microtextured substrates and microparticles used as *in situ* lenses for on-chip immunofluorescence amplification," *Anal. Chem.*, 85, 2064-2071, 2013.

## CONTACT

\* Hui Yang; hui.yang1002@gmail.com; Current Address: IMEC, Leuven, Belgium